Shahrood University of Technology

Journal of Mining and Environment (JME)

Journal homepage: www.jme.shahroodut.ac.ir

Iranian Society of Mining Engineering (IRSME)

Photocatalytic Treatment and Kinetic Study of Dye Wastewater by Synthesized ZnO Nanoparticles

Behnoosh Khataei[1]*, Farhad Qaderi[2], and Farzad Mosavat[2]

1. Civil and Environmental Engineering, Faculty of Geosciences Engineering, Arak University of Technology, Arak, Iran
2. Civil and Environmental Engineering, Faculty of Civil Engineering, Babol Noshirvani University of Technology, Babol, Iran

Article Info

Received 27 April 2024
Received in Revised form 4 June 2024
Accepted 25 June 2024
Published online 25 June 2024

DOI: 10.22044/jme.2024.14461.2717

Keywords

Photocatalyst
Dye Wastewater
Optimization
Kinetic
ZnO

Abstract

The increase in the number of factories, the industrialization of human life, and the increasing use of industrial paints have caused an increase in dye wastewater and consequent environmental pollution. Discharging wastewater containing the dyes mentioned above, which are often carcinogenic, is a severe threat to living organisms. In this research, a photocatalytic method (as an advanced oxidation method) using zinc oxide nanoparticles was investigated to treat the colored wastewater containing methylene blue. This type of nanoparticle is cheap (based on the used synthesis method), abundant and readily available, and low in toxicity. For this purpose, an evaluation of the optimal ratio between zinc acetate and polyvinylpyrrolidone for the synthesis of zinc oxide nanoparticles was carried out. Furthermore, the simultaneous decreasing and increasing effects of independent parameters (pH, irradiation time, methylene blue concentration, zinc acetate to PVP ratio) on the efficiency of the photocatalytic process and kinetic model were evaluated. The results showed that the best pollutant removal efficiency (91.7%) was obtained using the ratio of zinc acetate and polyvinylpyrrolidone equal to 33.67 in 60 minutes of irradiation time. This result shows that the lower ratio of zinc acetate to polyvinylpyrrolidone indicates higher dye removal.

1. Introduction

Dye wastewater is mainly caused by the combination of colored effluents from textile, dyeing, etc. factories with surface water. Textile wastewater is considered one of the significant factories in industrial wastewater treatment due to the high volume of wastewater and the existence of harmful environmental factors [1]. All industries need water directly or indirectly in a small or large amount, and according to the type of industry and the type of product, their water consumption should be almost clean water. The amount and volume of water consumed in some industries, including textile industries is a lot and finally, their by-product is polluted water with a very high pollution load. The output water in dyeing is also highly acidic and has a lot of minerals and dyes that cause turbidity and increase the TSS of wastewater [2,3]. The presence of dyes in textiles reduces the amount of oxygen and other gases dissolved in water, and as a result of entering the environment, disrupts the ecosystem of living organisms [4].

Methylene blue is one of the most important and widely used dyes in the dyeing and textile industries, It has a complex aromatic structure that is highly resistant to heat, chemicals, light, and even biological degradation [5]. Wastewater-containing dyes such as methylene blue are very dangerous for public health and the ecosystem. These substances affect water quality by reducing light penetration, creating eutrophication, and increasing turbidity and suspended matter [6]. On the other hand, due to the dry climatic conditions and the reduction of water resources in Iran, the need for safe water for drinking and agriculture is felt more than before. Besides, the preservation of water and soil resources from pollution by sewage has been taken into consideration [7].

✉ Corresponding author: b.khataei@arakut.ac.ir (B. Khataei)

There are two categories of traditional processes and advanced and new technologies to separate and remove pollutants from wastewater [8]. Traditional methods are based on the initial concentration of pollutants; extraction, absorption, distillation, total oxidation, biological degradation, and chemical oxidation can be mentioned [9]. New methods are divided into two categories: membrane separation technologies and photocatalytic processes [10]. Membrane [11], photooxidation [12,13], chemical oxidation, electrochemical oxidation [14], ultrasonic and photocatalytic method [15], adsorption and photocatalytic method [16], plasma [17], ozonation [18], and plasma-ozonation method [19] are among the advanced methods. The mentioned methods have disadvantages such as low efficiency (electrochemical and chemical extraction process), high cost (biological processes), production of excess pollutants, and the need for pretreatment [20-22]. It is also possible to remove colored pollutants from wastewater with various methods such as coagulation and flocculation, ion exchange, and hybrid processes like the use of absorbent and membrane filtration [23-25]. Most of the mentioned cases are inefficient, and expensive, with the volume of production sludge and dangerous by-products. However, the use of combined processes such as advanced oxidation (AOP) or photocatalytic decomposition with nanoparticles is preferred; Due to the non-production of dangerous secondary products, high efficiency, insensitivity to pollutants, recycling of absorbed pollutants, and reuse of treated wastewater. In many studies, different nanomaterials like TiO_2 [26-30], Fe_2O_3 [31], SiO_2 [32], WO_3 [33], ZnO [21,34], etc. have been successful in the decomposition of pollutants.

In photocatalytic treatment using nanoparticles, different pollutants in water and wastewater are decomposed by nanoparticles, under the influence of UV rays with the production of hydroxyl oxide radicals. In that, there are two types of covered and suspended reactors [35]. In the suspended reactor, nanoparticles are added to the colored wastewater in the form of powder, which is finally separated from the wastewater after the purification process. The most important problem of that is the recovery of catalysts. But in the method of covering and fixing nanoparticles on surfaces, in addition to solving the above problem, the pollutant can be separated and collected from the nanoparticles in the backwash process, so that the catalyst material can be used again. On the other hand, this technique can be applied in industrial and semi-industrial pilots to solve the problem of wastewater treatment [34]. Because in the photocatalytic process, catalysts use light to destroy organic substances and convert them into harmless ones [36]. This process depends on the intensity of the UV radiation and the duration of the radiation [37].

In several studies, the application of magnetic nano-photocatalysts to purify the water is reviewed [38,39]. The review of literature showed the application of nano-photocatalysts to remove the various dye like azo dye [40,41], methylene blue dye [42,43], Rhodamine-B dye [44,45], reactive blue dye [46,47], brilliant green dye [48,49], methyl red dye [50,51]. Some researchers investigated the destruction path of methylene blue in water by photocatalytic process. They used TiO_2 photocatalyst under UV light to purify the competing effluents of textile industries. They found that the photocatalyst can convert organic oxygen into CO_2 in water without heating. Removal of organic pollutants by photocatalytic method requires a lot of time and amount of light; To reduce the time, UV light is applied, which is dangerous and more expensive [5]. In another study, the photocatalytic decomposition of methylene blue dye using zinc oxide nanoparticles with a diameter below 50 nm and ultraviolet (UVA) radiation in a batch reactor was investigated. The results showed that the removal of methylene blue dye is directly related to the intensity of radiation. The best result of dye removal with a concentration of 5 mg/L was obtained in 60 minutes with 90% efficiency. They concluded that an increase in dye concentration led to a decrease in the rate of dye removal [21].

Some researchers evaluated the process of photocatalytic removal of methylene blue using nitrogen-silver nanoparticles doped on zinc oxide under the effect of visible light. Zinc oxide (CZ), silver doped on zinc oxide (CAZ), nitrogen-doped on zinc oxide (CNZ), and nitrogen-silver doped on zinc oxide (CANZ) were synthesized by chemical precipitation method. The results showed that for 20 mg/L methylene blue, the removal efficiency for each of CZ, CAZ, CNZ, and CANZ nanoparticles was 30, 35, 49, and 53%, respectively, in 135 minutes [52]. In research conducted in 2017, the photocatalytic effect of ZnO/Eu nanoparticles on the removal of methylene blue and methyl orange pollutants was evaluated. The structure of synthesized nanoparticles, as well as the efficiency of ZnO/Eu nanoparticles with different percentages of $Eu^{3+,}$ were investigated. The results showed that for 10 mg/L methylene blue and 1g/L photocatalyst, in 145 minutes and

under simulated sunlight, ZnO/Eu(1%) nanoparticles have the highest efficiency [53].

In a study conducted in 2018, the removal of Rhodamine-B dye from wastewater by ZnO nanoparticles and membrane filtration was investigated [54]. In another one, the photocatalytic removal of methylene blue and 4-nitrophenol was conducted using magnetic nanoparticles $ZnFe_2O_4$/ZnO/perlite under visible light. The tests performed to remove methylene blue with a concentration of 20 mg/L and 4-nitrophenol with a concentration of 10 mg/L have resulted in the removal efficiency of 97 and 67%, respectively. These efficiencies were achieved when 1 g/L nanoparticles during 150 minutes were exposed to visible light [55]. Furthermore, the photocatalytic removal of methylene blue by using doped manganese nanoparticles on zinc oxide under ultraviolet light was evaluated. The researchers investigated the effect of methylene blue concentration, nanoparticle concentration, and pH on the removal efficiency. In their study, 98% removal efficiency was achieved during 120 minutes of irradiation [56].

The main objective of the current study is to synthesize zinc oxide nanoparticles and apply them for the removal of methylene blue dye from colored wastewater during a photocatalytic process. For this purpose, the design of different mixtures in nanoparticle synthesis was investigated and the optimal conditions for this were defined. Then, the parameters influencing the photocatalytic purification process were evaluated, such as pH, initial dye concentration, ratio of zinc acetate to PVP, and irradiation time. Then, based on another goal of this research, studying the kinetics of the photocatalytic oxidation reaction determined the model compliance with the examined functions.

2. Materials and Methods

2.1. Methylene blue

Methylene blue is green and powdery, odorless, and solid at room temperature, and it becomes a blue solution by dissolving in water [57]. Methylene blue has a pH equal to 3 at a temperature of 20 ºC and is considered an acidic dye. Its chemical formula is $C_{16}H_{18}N_3SCl$ by 319.58 g/mol molecular weight. Its structure is shown in Figure 1. The methylene blue substance used in this research was produced by Merck, Germany. According to Figure 2, to find the absorption number of methylene blue, the wavelength entered in the spectrophotometer was 664 nm.

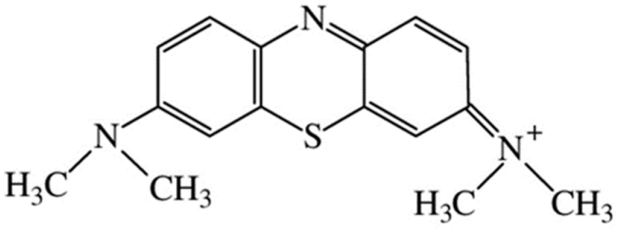

Figure 1. The structure of methylene blue [21]

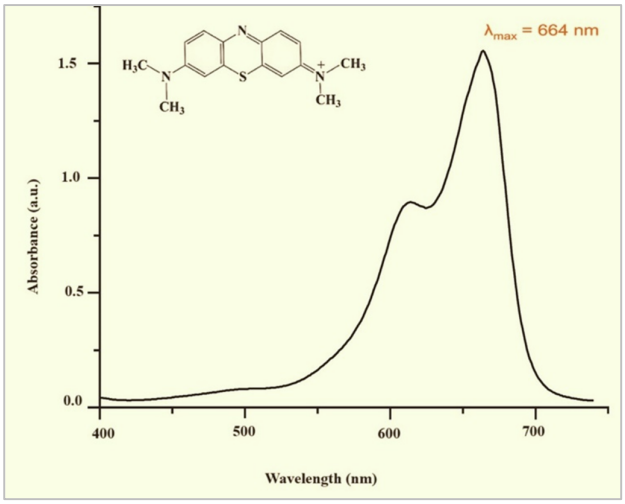

Figure 2. Wavelength curve of methylene blue

2.2. Zinc oxide

Zinc oxide has a crystalline and powdery structure that is hexagonally crystallized. It has unique electrical, optical, and chemical properties and is widely used in solar cells, ultraviolet lasers, transparent conductive layers, photocatalysts, and arresters [58]. Regarding the wide application of zinc oxide and its nanoparticles, many researchers synthesized its different morphologies by various methods. Its nanostructures with different morphologies include nanorods, nano bows, tower-shaped and flower-shaped nano wires, nano combs, nano rings, nano springs, etc. [59]. The diversity in the unique structure of zinc oxide shows that zinc nanoparticles are very valuable both in terms of properties and structure. Rod-shaped zinc oxide nanoparticle powder increases the quality of physical and chemical resistance of materials.

In the current study, Zn $(CH_3COO)_2.2H_2O$ and polyvinylpyrrolidone made by Merck (Germany) were provided. To make the nanomaterials, 5 mixing plans were used as follows: First, a constant amount of 0.11 g of PVP was dissolved in 11 cc of distilled water; different amounts of zinc acetate (0.035, 1.87, 3.7, 5.538 and 7.372 g) was dissolved in 11 cc of distilled water; After mixing the two solutions, by keeping the temperature constant at 70 ºC, and after the volume of the solution reaches 2 cc (finding a jelly state), it is placed in the oven at 110 °C for 12 hours and then at 300 ºC for 2 hours [35]. As in other studies, the best temperature for the synthesis of zinc oxide has been reported to be 300 ºC [60]. The nanoparticles with similar colors were produced in dark gray color according to Figure 3-a and after grinding, they reached the size of a nanoparticle (Figure 3-b).

(a) (b)

Figure 3. (a) Synthesized ZnO; (b) ZnO nanoparticle

2.3. Experimental design

Statistical methods have many advantages over traditional methods, as they allow rapid calculations and the ability to identify relationships between influencing factors. Various planning methods are currently used to reduce costs and increase test accuracy. One of the newest experimental design methods is response surface methodology (RSM). The central composition design (CCD) method, a subset of RSM, is the most well-known design method among quadratic methods and was first introduced by Box. RSM is used as one of the best multivariable methods in analytical optimization to determine the optimal model, experiments, and conditions. By placing the number of variables and the specified minimum and maximum range for each of the variables, the test matrix will be designed. Therefore, the amount of variables and the number of tests will be determined. When the number of variables is large, RSM has an advantage compared to other large-scale methods such as full factorial. This method is a set of statistical and mathematical techniques based on the fit of an equation and a polynomial based on experimental data, which should describe the behavior of a series of data that is organized with the purpose of statistical prediction. Therefore, the variable posing the most effect is selected, and the necessary decision must be made to determine which one of several experimental variables and their effects have significant effects on each other.

It is important to note that in this study, CCD was used by Design Expert 11 software to design the experiments and analyze the results. For this purpose, several pre-tests were conducted, and based on that, the range of independent variables was selected. Selected limits for independent variables are presented in Table 1. The independent parameters in examining the removal percentage of

dye pollutants are the concentration of methylene blue (mg/L), solution acidity (pH), ZnO/PVP ratio, and purification time (min), while the dependent variable is the removal percentage of dye pollutant. The software of Design Expert (ver. 11) was used to provide the model. After selecting the linear model, 30 experiments were designed (provided in Table 2).

Table 1. The range of independent variables to investigate the removal percentage of dye pollutant

Independent variable	Unit	range				
		-α	-1	0	+1	+α
pH	-	3.5	5	6.5	8	9.5
Time	min	20	30	40	50	60
Dye concentration	mg/L	10	15	20	25	30
ZnO/PVP	-	0.325	17	33.675	50.35	65.025

Table 2. The designed experiments

Run	A: pH	B: Time (min)	C: Dye conc. (mg/L)	D: ZnO/PVP	Removal efficiency (%)	Run	A: pH	B: Time (min)	C: Dye conc. (mg/L)	D: ZnO/PVP	Removal efficiency (%)
1	5	30	15	17	60	16	8	50	25	50.35	70.7
2	8	30	15	17	62.7	17	3.5	40	20	33.675	66
3	5	50	15	17	84	18	9.5	40	20	33.675	79.4
4	8	50	15	17	88.9	19	6.5	20	20	33.675	62.79
5	5	30	25	17	55	20	6.5	60	20	33.675	91.7
6	8	30	25	17	73	21	6.5	40	10	33.675	78.2
7	5	50	25	17	79	22	6.5	40	30	33.675	63
8	8	50	25	17	83	23	6.5	40	20	0.325	88.1
9	5	30	15	50.35	47	24	6.5	40	20	67.025	45
10	8	30	15	50.35	63	25	6.5	40	20	33.675	72.7
11	5	50	15	50.35	69.7	26	6.5	40	20	33.675	73
12	8	50	15	50.35	72.8	27	6.5	40	20	33.675	73.5
13	5	30	25	50.35	50.4	28	6.5	40	20	33.675	72.9
14	8	30	25	50.35	55.9	29	6.5	40	20	33.675	73.1
15	5	50	25	50.35	66.6	30	6.5	40	20	33.675	74

2.4. Experiments method

According to the experiments designed by the Design expert software (Table 2), first, the desired nanoparticles were fixed on the concrete cylinders. Then, the concrete sample was placed at a distance of 3 cm from the 250cc beaker (for the magnet's rotational movement) and methylene blue solution was poured and the pH of the solution was adjusted according to the test conditions. Next, it was placed in a closed and isolated chamber, on top of which UV lamps were installed at a distance of 12 cm from the surface of the sample. The schematic of the experimental reactor is displayed in Figure 4.

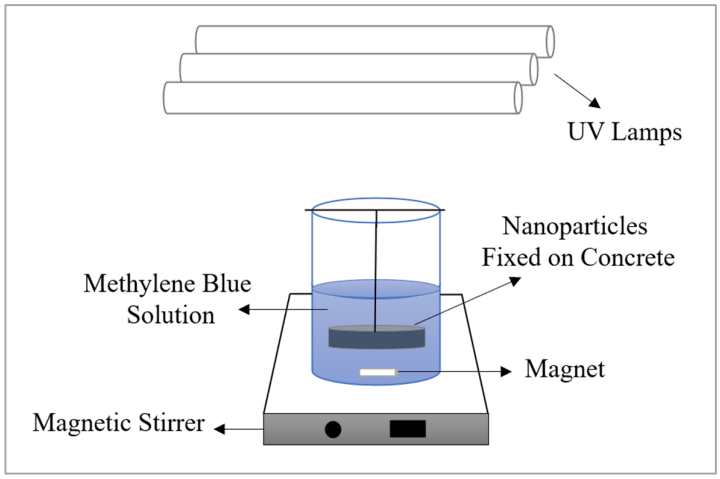

Figure 4. Schematic of the experimental reactor

2.5. Analysis tools

In continue, after passing the required irradiation time of the experiment and placing the sample in a centrifuge with a speed of 4000 rpm for 30 minutes (to settle the suspended particles), the residential concentration of dye was determined by a spectrophotometer device at the wavelength of 664 nm (the maximum absorption wavelength) [61]. Finally, the removal percentage of dye as the efficiency of the photodegradation process was calculated by Equation (1) [62].

$$\eta\ (\%) = \left(\frac{C_0 - C_t}{C_0}\right) \times 100 \qquad (1)$$

where η is the efficiency of process; C_0 and C_t are the initial and residual concentration at time t, respectively. In the end, the kinetics of the degradation process of methylene blue was studied. In this order, the test by optimum condition was repeated and dye residual concentration at different purification times was recorded in a constant dye initial concentration. The rate constant, k, was obtained by plotting the relationship between the initial concentration and the concentration at a certain time of methylene blue versus irradiation time.

3. Results and discussion

According to the results of GC-MS analysis, the degradation pathway of methylene blue is as follows. The aqueous structure of methylene blue was degraded to simple structures and then these two products were reduced to final products (displayed in Figure 5).

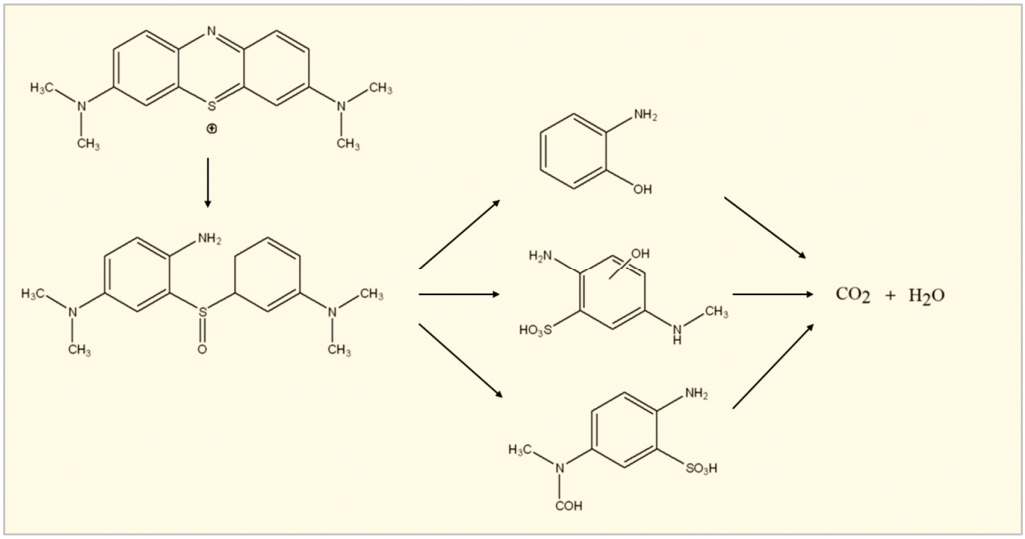

Figure 5. The possible destruction pathway of methylene blue

3.1. Effect of each variable on dye removal efficiency

In this section, the effect of each of the variables (pH, irradiation time, dye concentration, and ZnO/PVP ratio) on the removal efficiency of dye is examined (shown in Figure 6).

pH: According to the results (Figure 6-a), as pH increases, the amount of removal percentage also increases; that is, the more acidity of the solution goes towards alkaline, the removal percentage improves. In fact, with the increase in pH, the amount of negative hydroxyl is greater and the dye removal process is performed better. In other words, the solution pH is an important parameter in the photocatalytic reactions that occur on a specific surface. Because it is determinative of the surface charge properties of the photocatalyst and the size of formed aggregates [63]. Therefore, pH is important both in dye properties and in the reaction mechanisms that can contribute to dye degradation: attack by hydroxyl radicals, direct oxidation by holes, and direct reduction by electrons in the conductive band [64].

In the presence of photocatalysts, the photocatalytic process is thought to arise from electron-hole pairs formed on the surface of the semiconductor surface, possibly due to UV light [65]. Holes with high oxidation potential then directly oxidize the reactive dye or react with the OH^- to form hydroxyl radicals. The overall reaction between the photocatalyst and the reactive dye can be written as Equations (2) to (5) [65].

$$semiconductor + h\upsilon \rightarrow (semiconductor)(e_{CB}^- + h_{VB}^+) \quad (2)$$

$$h_{VB}^+ + dye \rightarrow dye^{\cdot +} (oxidation\ of\ the\ dye) \quad (3)$$

or

$$h_{VB}^+ + OH^- \rightarrow OH^{\cdot} \quad (4)$$

$$OH^{\cdot} + dye \rightarrow degradation\ of\ the\ dye \quad (5)$$

In the presence of ZnO, the photodegradation was significantly promoted at high pH. The lowest photodegradation at low pH is due to the photolysis of ZnO to Zn^{2+}, which occurs in acidic and neutral solutions, whereas efficient formation of hydroxyl radicals occurs in alkaline solutions. A similar result related to the effect of pH on the photocatalytic treatment has been reported by other researchers [66].

Dye concentration: as displayed in Figure 6-b, increasing the dye initial concentration led to the reduction in dye removal percentage. Because a greater number of dye molecules are absorbed on the surface of the photocatalyst and due to the reduction of direct contact and light penetration, it prevents the reaction between the dye molecules and the produced photonic holes. Subsequently, the production of hydroxyl radicals decreases [67]. Therefore, by increasing the initial concentration of dye, the number of dye molecules increases while the number of photocatalytic sites is constant [68]. Accordingly, more irradiation time and energy must be spent to remove the pollutant, and it becomes harder for light to reach the nanoparticles. Thus, the photocatalytic process is endangered, while the amount of both light and nanoparticles was considered constant. Other researchers also reported the same result about this parameter [21,69].

ZnO/PVP ratio: In continue, increasing the ratio of ZnO to PVP in the nanoparticle synthesis decreases the removal percentage (Figure 6-c). According to the conducted tests, the best temperature for nanoparticle synthesis is 300 ºC [35] and the best ratio is the lowest one. Because as much as the amount of PVP decreases, the energy required for burning and decomposition of zinc oxide decreases and it does not have the necessary efficiency to create nanoparticles. The amount of ZnO/PVP ratio to the synthesis of ZnO nanoparticles is investigated in some studies [70-72].

Irradiation time: According to Figure 6-d, since the irradiation time goes up, the removal percentage enhances, which is a natural occurrence; because more time is available to the zinc oxide catalysts to remove the methylene blue pollutant. In general, the effect of the important parameters affecting the photocatalytic process in the removal of different dyes is given in other researches [73-75].

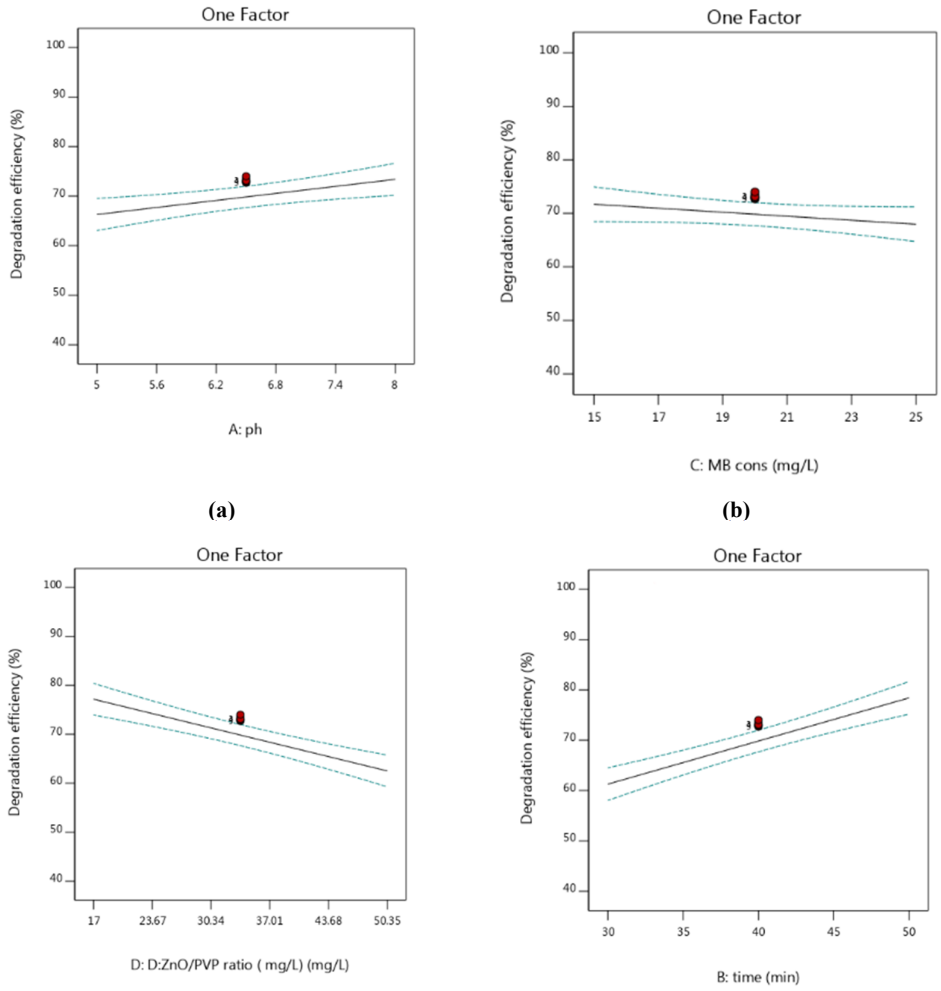

Figure 6. Effect of each variable on dye removal efficiency

3.2. Simultaneous effect of variables on dye removal efficiency

The simultaneous effect of pH and dye concentration is shown in Figure 7-a. In the condition of constant irradiation time, constant ZnO/PVP ratio, light intensity equal to 30 watts, and time equal to 21.5 minutes, as expected, by a decrease in dye concentration, the removal percent improves. In addition, with the increase in pH, the ability of nanoparticles to remove the pollutant and finally the removal percentage increases (as reported by [66]). Based on the results, it has the best removal efficiency at pH=8 and a pollutant concentration of 15 mg/L. According to Figure 7-b (the effect of both dye concentration and ZnO/PVP ratio), decreasing both dye concentration and ZnO/PVP ratio causes an increase in dye removal (in constant irradiation time and light intensity of 30 watts). How the dye concentration works in the photocatalytic process was explained in the previous section. This positive and direct impact has also been observed in another research [76]. The maximum amount of dye removal occurred in a dye concentration of 15 mg/L and ZnO/PVP ratio of 17. To investigate the concurrent effect of pH and ZnO/PVP ratio, the other variables like irradiation time and light intensity were kept constant. It is obtained that in similar conditions, increasing the pH and decreasing the ZnO/PVP ratio improve the dye removal amount (Figure 7-c). The highest removal efficiency was related to pH=8 and ZnO/PVP ratio equal to 17. About the effect of irradiation time and ZnO/PVP ratio simultaneously, it was observed that by bypassing the time and increasing the ZnO/PVP ratio, the removal efficiency was raised. So, an irradiation time of 50 minutes and a ZnO/PVP ratio equal to 17 resulted in the best situation of dye removal

(displayed in Figure 7-d). In constant pH and ZnO/PVP ratio, the effect of both variables of time and dye concentration was evaluated and shown in Figure 6-e. Based on that, irradiation time and dye concentration have positive and negative effects on the removal efficiency, respectively. Therefore, a time of 50 minutes and 15 mg/L dye led to the best removal efficiency. Figure 6-f represents the concurrent effect of irradiation time and pH at constant dye concentration and ZnO/PVP ratio. In this way, increase in both time and pH results in an improvement in dye removal. The best conditions were obtained at pH=8 and 60 minutes.

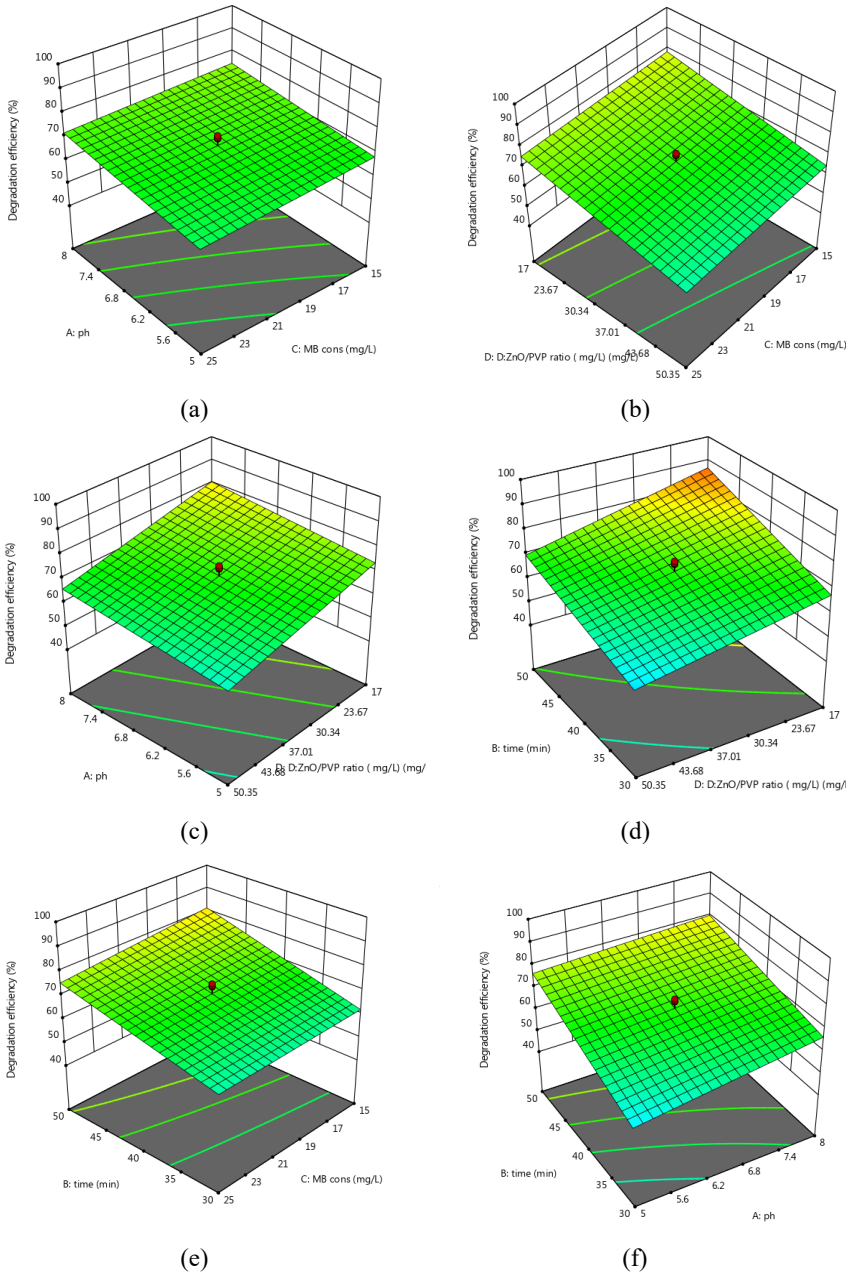

Figure 7. Simultaneous effect of variables on dye removal efficiency

3.3. Interaction between variables

Figure 8-a shows the decreasing and increasing effect of irradiation time and acidity variables, on each other's efficiency in dye removal. Based on that, by increasing the time, the effect of acidity on the removal percentage decreases. While, according to Figure 8-b, an increase in dye

concentration leads to an increase in the effect of irradiation time on the removal efficiency. In continuing, decreasing and increasing the effect of the ZnO/PVP ratio and time on each other's removal efficiency is presented in Figure 8-c. By increasing the ZnO/PVP ratio, no variation is observed in the effect of irradiation time on dye removal. Thus, no interaction between the above variables was resulted.

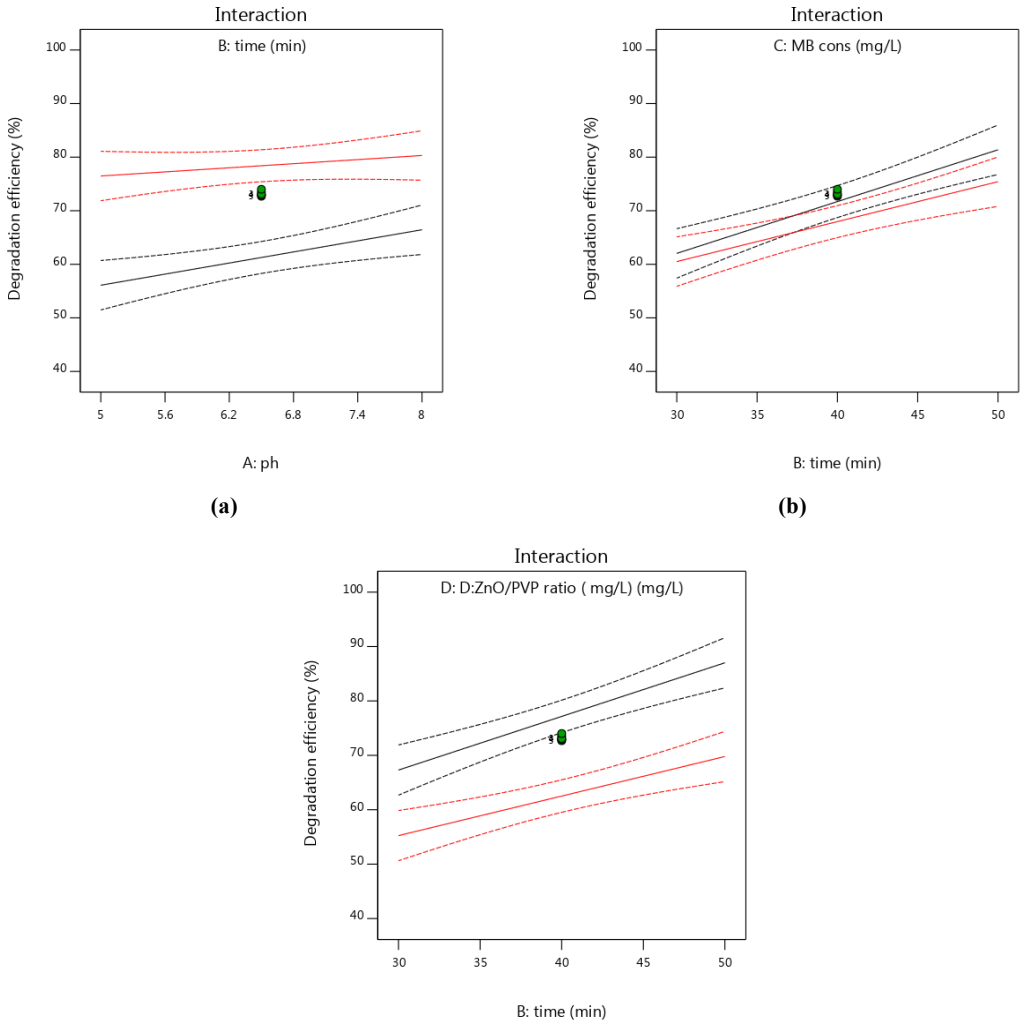

Figure 8. Interaction between variables

3.4. Suggested model, optimum condition, and validation of the model

The proposed model by software is presented in Equation (6).

$$\text{Degradation efficiency (\%)} = -13.94 + 6.71\ \text{pH} + 2.26\ \text{time} + 0.51\ \text{MB conc.} - 0.12\ \text{ZnO/PVP ratio} - 0.10\ \text{pH} * \text{time} - 0.02\ \text{time} * \text{MB conc.} - 0.0077586206896552\ \text{time} * \text{ZnO/PVP ratio} \quad (6)$$

In the resulting model, R^2 and p-value of the model were obtained at about 0.9026 and <0.0001 (significant) respectively, which confirms the validity of the proposed model. Also, the lack of fit of the model is statistically insignificant (> 0.05), approving the compatibility of the suggested model with the experimental data. Figure 9 shows the accuracy and validity of the proposed model by RSM. In that, the predicted amount of response by the suggested model of RSM is displayed versus

the actual amount of response by the experiments. The proximity and accumulation of the predicted points to the inclined line (which represents the actual value obtained from the designed experiments) indicate the effectiveness of the model for predicting the behavior of the response variable. By the results, the amount of affecting parameters on removal efficiency of dye under optimal conditions was obtained as pH=6.5, irradiation time of 60 minutes, dye concentration of 20 mg/L, and ZnO/PVP ratio of 33.67. In this way, the maximum amount of response (removal efficiency of dye) was achieved at about 91.7%. It should be noted that these conditions were checked through the confirmation test and the validation of the model was evaluated and confirmed.

In continue, the resulting optimum conditions have been compared with other studies by application of various nanoparticles in the photocatalytic treatment of dyes (summarized in Table 3) in which, the efficiency of the synthesized ZnO nanoparticles in removing the methylene blue has been well demonstrated.

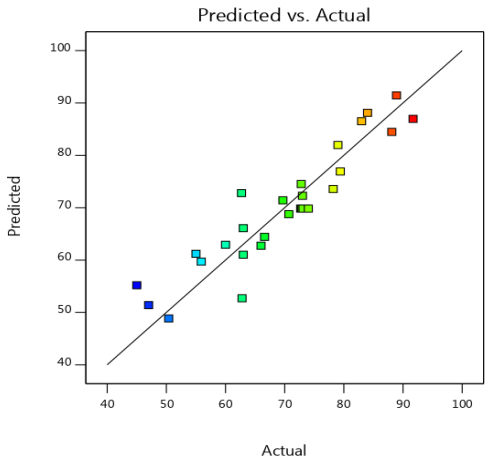

Figure 9. Predicted vs. actual amount of response variable

Table 3. The comparison of obtained results with other studies

No.	Nanoparticles	Dye	Conditions	Removal efficiency	Ref.
1	ZnO	methylene blue	60 minutes	90%	[20]
2	N-Ag doped on ZnO	methylene blue	135 minutes	53%	[52]
3	ZnO/Eu	methylene blue methyl orange	10 mg/L dye, 1g/L ZnO/Eu, 145 minutes, ZnO/Eu (1-10%)	89% 93%	[53]
4	ZnO	rhodamine B	membrane filtration, 90 min	96%	[54]
5	TiO_2	azo dye	50 mg/L dye, 9.5 h	69.7%	[26]
6	$ZnFe_2O_4$/ZnO/perlite	methylene blue 4-nitrophenol	20 mg/L methylene blue 10 mg/L 4-nitrophenol	97% 67%	[55]
7	Mg doped on ZnO	methylene blue	120 minutes	98%	[56]
8	ZnO	methylene blue methyl orange Rhodamine B	60 min 180 min 180 min	100% 85% 92%	[77]
9	Ag	methylene blue	100 mg/L dye, 180 min	96.5%	[78]
10	MgO	methylene blue rhodamine B	150 min 180 min	98% 94%	[79]
11	TiO_2	acid orange	9.5 h	89%	[30]
12	TiO_2	methylene blue	3.15×10^{-15} M dye 7.98 h	96.6%	[27]
13	ZnO	methylene blue	60 min	91.7%	Present study

3.5. The kinetics of the photocatalytic process

The reaction kinetics provides valuable information about the rate and mechanism of the reaction that indicates the degradation of contaminants to the products. To determine the most appropriate kinetic model for the data of the photocatalytic process, three types of zero-order, first-order, and second-order kinetic equations were used in optimal conditions. The relations governing the considered reaction are presented in Equations (7) to (9) [80].

$$C_0 - C_t = k_0 t \quad (7)$$

$$Ln\left(\frac{C_0}{C_t}\right) = k_1 t \quad (8)$$

$$\frac{1}{C_t} - \frac{1}{C_0} = k_2 t \quad (9)$$

where k_0 ($mol.L^{-1}.min^{-1}$), k_1 (min^{-1}), and k_2 ($L.mol^{-1}.min^{-1}$) are the reaction rate constants of the zero-order, first-order and second-order reaction, respectively; C_0 is the initial concentration of dye;

C_t is the residual concentration of dye at time t (min). K was obtained by plotting the relationship between the initial concentration and the concentration at a given irradiation time of methylene blue against the irradiation time assuming the relations of zero-order, first-order, and second-order reaction as shown in Figure 10. Furthermore, the obtained amount of reaction rate constant (k) and correlation coefficient (R^2) related to investigated reactions are summarized in Table 4.

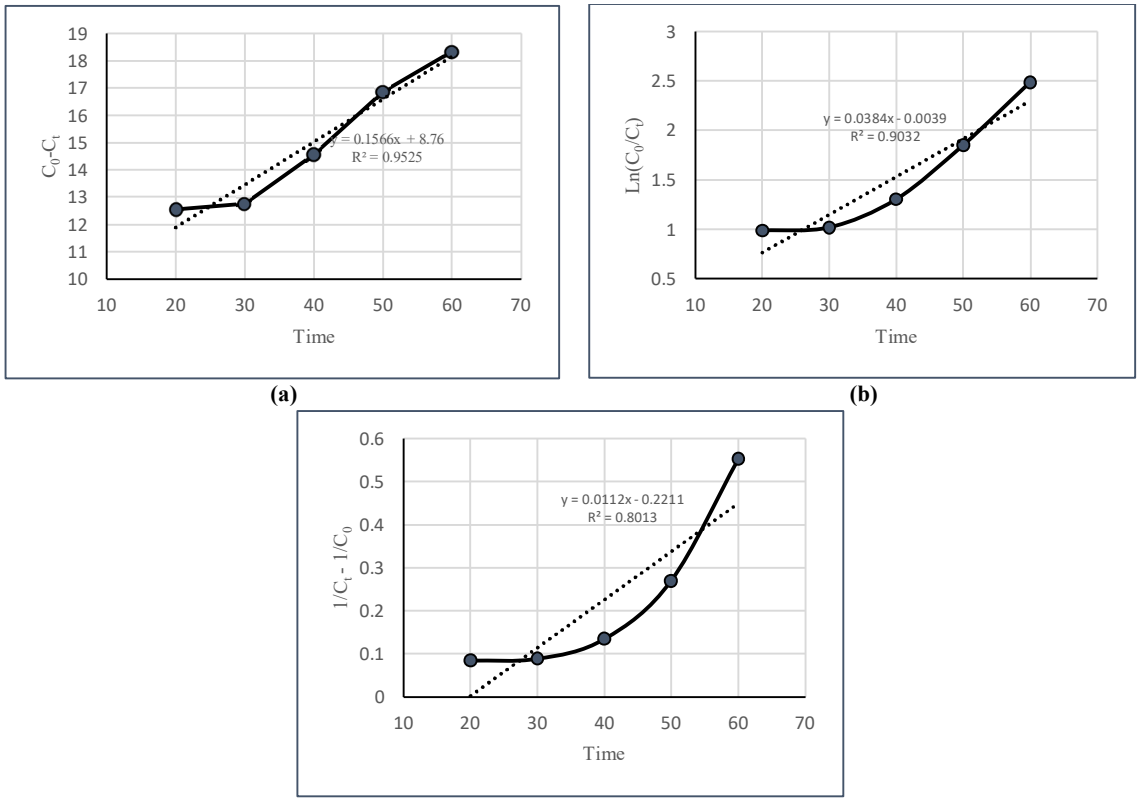

Figure 10. Kinetic models of photocatalytic dye removal based on (a) zero-order, (b) first-order, (c) second-order reaction

Table 4. The obtained coefficients of kinetic models

No	Rate of reaction	k	R^2
1	Zero-order reaction	k_0=0.1566	0.9525
2	First-order reaction	k_1=0.0384	0.9032
3	Second-order reaction	k_2=0.0112	0.8013

As a result, the photocatalytic process of removing methylene blue dye using ZnO nanoparticles is more consistent with the zero-order kinetic model (Figure 10-a) by a higher correlation coefficient value (R^2=0.95). A similar study using a photocatalytic process by TiO_2 and ZnO nanoparticles to remove organic dyes reported the process compliance with a zero-order kinetic model [81]. On the other hand, by comparison of first-order and second-order kinetic, photodegradation reaction followed the first-order kinetic model in better accordance (by comparing Figures 10-b and 10-c, and related correlation coefficients). This result was also achieved in other studies on acid blue 113 dye removal by a photocatalytic process using zinc oxide-kaolin nanocomposite [82] as well as rhodamine B and methylene blue dye removal by MgO nanoparticles [79].

4. Conclusions

The growth of factories, the industrialization of human life, and the extensive use of industrial colors have caused an increase in colored wastewater and consequently environmental pollution. Discharging wastewater containing the aforementioned dyes, which are often

carcinogenic, is a grave threat to living organisms. In addition, these wastewaters have low degradability and high toxicity. Methylene blue dye is a common dye used in textile, rubber, paper, leather, and pharmaceutical industries. Already many methods such as adsorption, and chemical and biological oxidation have been employed for pollutant removal from wastewater. Additionally, new methods like membrane separation technologies and photocatalytic processes are more applicable. However, nanomaterials have widespread usage in wastewater treatment due to their features of being biodegradable, non-toxic and having excellent water purification capabilities. Zinc oxide nanoparticles are also an abundant, relatively cheap (according to the used synthesis method), and very low toxicity substance that has wide applications in the photocatalytic process. Thus, in this research, by using synthesized ZnO nanoparticles, the decomposition of methylene blue dye is investigated during the photocatalytic process. To achieve this objective, effective parameters in removing methylene blue dye were considered as the mixing ratio of nanoparticle components, pH, irradiation time, and methylene blue concentration to investigate the optimal conditions and improve the performance of the photocatalytic process. The results showed that solution pH is one of the most effective parameters in the removal of dye. Since ZnO nanoparticles have performed better for the removal process in the alkaline solution. 30 watts power range of UV lamp is suitable for photocatalytic treatment of dye. The maximum removal efficiency (91.7%) of the purification process was obtained at optimum conditions such as pH=6.5, irradiation time of 60 minutes, initial dye concentration of 20 mg/L, and zinc acetate to PVP ratio of 33.67. This result also showed that the photocatalytic treatment of methylene blue using ZnO nanoparticles is more consistent with the zero-order kinetic model by 0.95 correlation coefficient. Accordingly, the results contribute to the improvement of effective and useful treatment strategies specifically photocatalytic processes in dye and other organic contaminant removal. In future studies, other methods for synthesizing zinc oxide nanoparticles could be investigated.

References

[1]. Kishor, R., Purchase, D., Ferreira, L., Mulla, S., Bilal, M., & Bharagava, R. (2020). Environmental and health hazards of textile industry wastewater pollutants and its treatment approaches. In C. Hussain (Ed.), *Handbook of Environmental Materials Management* (pp. 1-24). Springer Nature.

[2]. Islam, M., & Mostafa, M. (2018). Textile dyeing effluents and environment concerns-a review. *Journal of Environmental Science and Natural Resources*, 11. 144-131, (2-1).

[3]. Wang, Z., Xue, M., Huang, K., & Liu, Z. (2011). Textile dyeing wastewater treatment. *Advances in treating textile effluent*, *5*, 91-116 .

[4]. Mehra, S., Singh, M., & Chadha, P. (2021). Adverse impact of textile dyes on the aquatic environment as well as on human beings. *Toxicol. Int*, *28*(2), 165 .

[5]. Lachheb, H., Puzenat, E., Houas, A., Ksibi, M., Elaloui, E., Guillard, C., & Herrmann, J-.M. (2002). Photocatalytic degradation of various types of dyes (Alizarin S, Crocein Orange G, Methyl Red, Congo Red, Methylene Blue) in water by UV-irradiated titania. *Applied Catalysis B: Environmental*, *39*(1), 75-90 .

[6]. Berradi, M., Hsissou, R., Khudhair, M., Assouag, M., Cherkaoui, O., El Bachiri, A., & El Harfi, A. (2019). Textile finishing dyes and their impact on aquatic environs. *Heliyon*, *5*, (11).

[7]. Akhtar, N., Syakir Ishak, M. I., Bhawani, S. A., & Umar, K. (2021). Various natural and anthropogenic factors responsible for water quality degradation: A review. *Water*, *13*(19), 2660 .

[8]. Hao, O. J., Kim, H., & Chiang, P.-C. (2000). Decolorization of wastewater. *Critical reviews in environmental science and technology*, *30*(4), 449-505 .

[9]. Bhargava, S. K., Tardio, J., Prasad, J., Föger, K., Akolekar, D. B., & Grocott, S. C. (2006). Wet oxidation and catalytic wet oxidation. *Industrial & engineering chemistry research*, *45*(4), 1221-1258 .

[10]. Mozia, S. (2010). Photocatalytic membrane reactors (PMRs) in water and wastewater treatment. A review. *Separation and purification technology*, *73*(2), 71-91 .

[11]. Zhang, Q., Cheng, X., Zheng, C., Feng, X., Qiu, G., Tan, W., & Liu, F. (2011). Roles of manganese oxides in degradation of phenol under UV-Vis irradiation: adsorption, oxidation, and photocatalysis. *Journal of Environmental Sciences*, *23*(11), 1904-1910 .

[12]. Han, D.-H., Cha, S.-Y., & Yang, H.-Y. (2004). Improvement of oxidative decomposition of aqueous phenol by microwave irradiation in UV/H_2O_2 process and kinetic study. *Water Research*, *38*(11), 2782-2790 .

[13]. Veeresh, G. S., Kumar, P., & Mehrotra, I. (2005). Treatment of phenol and cresols in upflow anaerobic sludge blanket (UASB) process: a review. *Water Research*, *39*(1), 154-170 .

[14]. Kargari, A., & Mohammadi, S. (2015). Evaluation of phenol removal from aqueous solutions by UV, RO, and UV/RO hybrid systems. *Desalination and water treatment*, *54*(6), 1612-1620 .

[15]. Khataei, B., & Ghaderi, M. (2019). Optimizing the Annealing Effect of Zn/Ac Nanoparticle Synthesis on Dye Wastewater Treatment by Combination of Ultrasonic and

Photocatalytic Methods. *Determinations in Nanomedicine and Nanotechnology*, *1*(3), 1-3.

[16]. Miranzadeh, M., Afshari, F., Khataei, B., & Kassaee, M. (2020). Adsorption and photocatalytic removal of arsenic from water by a porous and magnetic nanocomposite: Ag/TiO_2/Fe_3O_4@ GO. *Adv. J. Chem. A*, *3*(4), 408-421 .

[17]. Ahmadi, K., Qaderi, F., Rahmaninejad, M., & Shidpour, R. (2024). Sustainable nanocomposite of PAC/Fe_3O_4-coated geotextile using plasma treatment technique for phenol adsorption application. *Geoenergy Science and Engineering*, 212882 .

[18]. Yaseri, A. M., Qaderi, F., & Khataei, B. (2023). Treatment of wastewater containing hard degradable pollutants through the advanced oxidation process (ozonation). *Journal of Civil and Environmental Engineering* .

[19]. Khourshidi, A., & Qaderi, F. (2023). Optimization of p-nitrophenol-contaminated water by non-thermal plasma technology and ozonation by response surface method. *Modares Civil Engineering journal*, *23*(5), 0-0 .

[20]. Kakavandi, B., Rezaei Kalantary, R., Esrafili, A., Jonidi Jafari, A., & Azari, A. (2013). Isotherm, kinetic and thermodynamic of Reactive Blue 5 (RB5) dye adsorption using Fe_3O_4 nanoparticles and activated carbon magnetic composite. *Journal of Color Science and Technology*, *7*(3), 237-248 .

[21]. Masombaigi, H., Rezaee, A., & Nasiri, A. (2009). Photocatalytic degradation of Methylene Blue using ZnO nano-particles. *Iranian Journal of Health and Environment*, *2*(3), 188-195 .

[22]. Yu, J.-G., Zhao, X.-H., Yang, H., Chen, X.-H., Yang, Q., Yu, L.-Y., Jiang, J.-H., & Chen, X.-Q. (2014). Aqueous adsorption and removal of organic contaminants by carbon nanotubes. *Science of the Total Environment*, *482*, 241-251 .

[23]. Chong, M. N., & Jin, B. (2012). Photocatalytic treatment of high concentration carbamazepine in synthetic hospital wastewater. *Journal of Hazardous Materials*, *199*, 135-142 .

[24]. Liu, X., Chen, Z., Chen, Z., Megharaj, M., & Naidu, R. (2013). Remediation of Direct Black G in wastewater using kaolin-supported bimetallic Fe/Ni nanoparticles. *Chemical engineering journal*, *223*, 764-771 .

[25]. Otton, J. K. (2006). Environmental aspects of produced-water salt releases in onshore and coastal petroleum-producing areas of the conterminous US-a bibliography. *US Geological Survey Reston*, VA, USA .

[26]. Ayati, B. (2018). Modeling of a photocatalytic baffled reactor to degrade colored wastewater using response surface methodology. *Modares Civil Engineering journal*, *18*(1), 113-122 .

[27]. Ghasemi, A. H., Zoqi, M. J., & Zanganeh Ranjbar, P. (2024). Enhanced photocatalytic degradation of methylene blue using a novel counter-rotating disc reactor. *Frontiers in Chemistry*, *12*, 1335180 .

[28]. Rabieian, M., & Qaderi, F. (2024). Optimizing Hybrid Photocatalytic-ozonation for Offshore Produced Water Treatment. *Journal of Mining and Environment*, *15*(1), 239-259 .

[29]. Ranjbar, P. Z., Ayati, B., & Ganjidoust, H. (2019). Kinetic study on photocatalytic degradation of Acid Orange 52 in a baffled reactor using TiO_2 nanoparticles. *Journal of Environmental Sciences*, *79*, 213-224 .

[30]. Ranjbar, P. Z., Ayati, B., & Ganjidoust, H. (2022). Textile dye degradation in a novel photocatalytic baffled reactor using immobilised TiO2 nanoparticles. *International Journal of Environment and Waste Management*, *29*(3), 241-261 .

[31]. Kusior, A., Michalec, K ,.Jelen, P., & Radecka, M. (2019). Shaped Fe_2O_3 nanoparticles–synthesis and enhanced photocatalytic degradation towards RhB. *Applied surface science*, *476*, 342-352 .

[32]. Hu, C., Tang, Y., Jimmy, C. Y & ,.Wong, P. K. (2003). Photocatalytic degradation of cationic blue X-GRL adsorbed on TiO_2/SiO_2 photocatalyst. *Applied Catalysis B: Environmental*, *40*(2), 131-140 .

[33]. Hayat, K., Gondal, M., Khaled, M., Yamani, Z., & Ahmed, S. (2011). Laser induced photocatalytic degradation of hazardous dye (Safranin-O) using self synthesized nanocrystalline WO_3. *Journal of Hazardous Materials*, *186*(2-3), 1226-1233 .

[34]. Malayeri, H. Z., Ayati, B., & Ganjidoust, H. (2014). Photocatalytic phenol degradation by immobilized nano ZnO: intermediates & key operating parameters. *Water Environment Research*, *86*(9), 771-778 .

[35]. De Lasa, H. I., Serrano, B., & Salaices, M. (2005). *Photocatalytic reaction engineering* (Vol. 590). Springer .

[36]. Weon, S., He, F., & Choi, W. (2019). Status and challenges in photocatalytic nanotechnology for cleaning air polluted with volatile organic compounds: visible light utilization and catalyst deactivation. *Environmental Science: Nano*, *6*(11), 3185-3214 .

[37]. Chiou, C.-H., Wu, C.-Y., & Juang, R.-S. (2008). Influence of operating parameters on photocatalytic degradation of phenol in UV/TiO_2 process. *Chemical engineering journal*, *139*(2), 322-329 .

[38]. Gómez-Pastora, J., Dominguez, S., Bringas, E., Rivero, M. J., Ortiz, I., & Dionysiou, D. D. (2017). Review and perspectives on the use of magnetic nanophotocatalysts (MNPCs) in water treatment. *Chemical engineering journal*, *310*, 407-427 .

[39]. Liu, S.-Q. (2012). Magnetic nano-photocatalysts: preparation, structure, and application. *Environmental Chemistry for a Sustainable World: Volume 1: Nanotechnology and Health Risk*, 99-117 .

[40]. Karimi, F., Zare, N., Jahanshahi, R., Arabpoor, Z., Ayati, A., Krivoshapkin, P., Darabi, R., Dragoi, E. N., Raja, G. G., & Fakhari, F. (2023). Natural waste-derived nano photocatalysts for azo dye degradation. *Environmental Research*, 117202 .

[41]. Mohaghegh, N., Tasviri, M., Rahimi, E., & Gholami, M. R. (2014). Nano sized ZnO composites: Preparation, characterization and application as photocatalysts for degradation of AB92 azo dye. *Materials science in semiconductor processing*, *21*, 167-179 .

[42]. Fouda, A., Salem, S. S., Wassel, A. R., Hamza, M. F., & Shaheen, T. I. (2020). Optimization of green biosynthesized visible light active CuO/ZnO nano-photocatalysts for the degradation of organic methylene blue dye. *Heliyon*, *6,* (9).

[43]. Padmapriya, G., Manikandan, A., Krishnasamy, V., Jaganathan, S. K., & Antony, S .A. (2016). Spinel NixZn1− xFe$_2$O$_4$ (0.0≤ x≤ 1.0) nano-photocatalysts: synthesis, characterization and photocatalytic degradation of methylene blue dye. *Journal of Molecular Structure*, *1119*, 39-47 .

[44]. Lops, C., Ancona, A., Di Cesare, K., Dumontel, B., Garino, N., Canavese, G., Hérnandez, S., & Cauda, V. (2019). Sonophotocatalytic degradation mechanisms of Rhodamine B dye via radicals generation by micro-and nano-particles of ZnO. *Applied Catalysis B: Environmental*, *243*, 629-640 .

[45]. Mahlambi, M. M., Mishra, A. K., Mishra, S. B., Krause, R. W., Mamba, B. B., & Raichur, A. M. (2012). Comparison of rhodamine B degradation under UV irradiation by two phases of titania nano-photocatalyst . *Journal of thermal analysis and calorimetry*, *110*(2), 847-855 .

[46]. Dhiman, P., Mehta, T., Kumar, A., Sharma, G., Naushad, M., Ahamad, T., & Mola, G. T. (2020). Mg0. 5NixZn0. 5-xFe$_2$O$_4$ spinel as a sustainable magnetic nano-photocatalyst with dopant driven band shifting and reduced recombination for visible and solar degradation of Reactive Blue-19. *Advanced Powder Technology*, *31*(12), 4585-4597 .

[47]. Samsudin, E. M., Goh, S. N., Wu, T. Y., Ling, T. T., Hamid, S. B. A., & Juan, J. C. (2015). Evaluation on the photocatalytic degradation activity of reactive blue 4 using pure anatase nano-TiO$_2$. *Sains Malaysiana*, *44*(7), 1011-1019 .

[48]. Jeyaraj, M., Atchudan, R., Pitchaimuthu, S., Edison, T. N. J. I., & Sennu, P. (2021). Photocatalytic degradation of persistent brilliant green dye in water using CeO$_2$/ZnO nanospheres. *Process Safety and Environmental Protection*, *156*, 457-464 .

[49]. Mahmood, K., Amara, U., Siddique, S., Usman, M., Peng, Q., Khalid, M., Hussain, A., Ajmal, M., Ahmad, A., & Sumrra, S. H. (2022). Green synthesis of Ag@ CdO nanocomposite and their application towards brilliant green dye degradation from wastewater. *Journal of Nanostructure in Chemistry*, 1-13 .

[50]. Narayan, R. B., Goutham, R., Srikanth, B., & Gopinath, K. (2018). A novel nano-sized calcium hydroxide catalyst prepared from clam shells for the photodegradation of methyl red dye. *Journal of Environmental Chemical Engineering*, *6*(3), 3640-3647 .

[51]. Saghi, M., Shokri, A., Arastehnodeh, A., Khazaeinejad, M., & Nozari, A. (2018). The photo degradation of methyl red in aqueous solutions by α-Fe$_2$O$_3$/SiO$_2$ nano photocatalyst. *Journal of Nanoanalysis*, *5*(3), 163-170 .

[52]. Welderfael, T., Pattabi, M., & Pattabi, R. M. (2016). Photocatalytic activity of Ag-N co-doped ZnO nanorods under visible and solar light irradiations for MB degradation. *Journal of Water Process Engineering*, *14*, 117-123 .

[53]. Trandafilović, L. V., Jovanović, D. J., Zhang, X., Ptasińska, S., & Dramićanin, M. (2017). Enhanced photocatalytic degradation of methylene blue and methyl orange by ZnO: Eu nanoparticles. *Applied Catalysis B: Environmental*, *203*, 740-752 .

[54]. Naresh Yadav, D., Anand Kishore, K., Bethi, B., Sonawane, S. H., & Bhagawan, D. (2018). ZnO nanophotocatalysts coupled with ceramic membrane method for treatment of Rhodamine-B dye waste water. *Environment, Development and Sustainability*, *20*, 2065-2078 .

[55]. Bayat, R ,.Derakhshi, P., Rahimi, R., Safekordi, A. A., & Rabbani, M. (2019). A magnetic ZnFe$_2$O$_4$/ZnO/perlite nanocomposite for photocatalytic degradation of organic pollutants under LED visible light irradiation. *Solid State Sciences*, *89*, 167-171 .

[56]. Chanu, L. A., Singh, W. J., Singh, K. J., & Devi, K. N. (2019). Effect of operational parameters on the photocatalytic degradation of Methylene blue dye solution using manganese doped ZnO nanoparticles. *Results in Physics*, *12*, 1230-1237 .

[57]. Aksu, Z., Ertuğrul, S., & Dönmez, G. (2010). Methylene Blue biosorption by Rhizopus arrhizus: Effect of SDS (sodium dodecylsulfate) surfactant on biosorption properties. *Chemical engineering journal*, *158*(3), 474-481 .

[58]. Schropp, R., & Madan, A. (1989). Properties of conductive zinc oxide films for transparent electrode applications prepared by rf magnetron sputtering. *Journal of applied physics*, *66*(5), 2027-2031 .

[59]. Kumar, G. A., Reddy, M. R., & Reddy, K. N. (2012). Effect of annealing on ZnO thin films grown on quartz substrate by RF magnetron sputtering. Journal of Physics: Conference Series,.

[60]. Khalegh, R., & Qaderi, F. (2019). Optimization of the effect of nanoparticle morphologies on the cost of dye wastewater treatment via ultrasonic/photocatalytic hybrid process. *Applied Nanoscience*, *9*, 1869-1889 .

[61]. Lundstedt, T., Seifert, E., Abramo, L., Thelin, B., Nyström, Å., Pettersen, J., & Bergman, R. (1998). Experimental design and optimization. *Chemometrics and intelligent laboratory systems*, *42*(1-2), 3-40 .

[62]. Molea, A., Popescu, V., Rowson, N. A., & Dinescu, A. M. (2014). Influence of pH on the formulation of TiO$_2$ nano-crystalline powders with high photocatalytic activity. *Powder technology*, *253*, 22-28 .

[63]. Haque, M., & Muneer, M. (2007). Photodegradation of norfloxacin in aqueous suspensions of titanium dioxide. *Journal of Hazardous Materials*, *145*(1-2), 51-57 .

[64]. Selvaraj, V., Karthika, T. S., Mansiya, C., & Alagar, M. (2021). An over review on recently developed techniques, mechanisms and intermediate involved in the advanced azo dye degradation for industrial applications. *Journal of Molecular Structure*, *1224*, 129195 .

[65]. Li, H., Fei, G. T., Fang, M., Cui ,P., Guo, X., Yan, P., & De Zhang, L. (2011). Synthesis of urchin-like Co_3O_4 hierarchical micro/nanostructures and their photocatalytic activity. *Applied surface science*, *257*(15), 6527-6530 .

[66]. Daneshvar, N., Salari, D., & Khataee, A. (2003). Photocatalytic degradation of azo dye acid red 14 in water: investigation of the effect of operational parameters. *Journal of Photochemistry and Photobiology A: Chemistry*, *157*(1), 111-116 .

[67]. Mahdizadeh, F., & Aber, S. (2015). Treatment of textile wastewater under visible LED lamps using CuO/ZnO nanoparticles immobilized on scoria rocks. *RSC Advances*, *5*(92), 75474-75482 .

[68]. Thejaswini, T., Mohan, A. M., Sompalli, N. K., & Deivasigamani, P. (2019). Assessment of tailor-made mesoporous metal doped TiO_2 monolithic framework as fast responsive visible light photocatalysts for environmental remediation applications. *Inorganic Chemistry Communications*, *110*, 107593 .

[69]. Nuengmatcha, P., Porrawatkul, P., Chanthai, S., Sricharoen, P., & Limchoowong, N. (2019). Enhanced photocatalytic degradation of methylene blue using Fe_2O_3/graphene/CuO nanocomposites under visible light. *Journal of Environmental Chemical Engineering*, *7*(6), 103438 .

[70]. Gutul, T., Rusu, E., Condur, N., Ursaki, V., Goncearenco, E., & Vlazan, P. (2014). Preparation of poly (N-vinylpyrrolidone)-stabilized ZnO colloid nanoparticles. *Beilstein journal of nanotechnology*, *5*(1), 402-406 .

[71]. Ilegbusi, O. J., & Trakhtenberg, L. (2013). Synthesis and conductometric property of sol-gel-derived ZnO/PVP nano hybrid films. *Journal of materials engineering and performance*, *22*, 911-915 .

[72]. Naveed Ul Haq, A., Nadhman, A ,.Ullah, I., Mustafa, G., Yasinzai, M., & Khan, I. (2017). Synthesis approaches of zinc oxide nanoparticles: the dilemma of ecotoxicity. *Journal of Nanomaterials*, *2017* .

[73]. Akpan, U. G., & Hameed, B. H. (2009). Parameters affecting the photocatalytic degradation of dyes using TiO_2-based photocatalysts: a review. *Journal of Hazardous Materials*, *170*(2-3), 520-529 .

[74]. Kumar, A., & Pandey, G. (2017). A review on the factors affecting the photocatalytic degradation of hazardous materials. *Mater. Sci. Eng. Int. J*, *1*(3), 1-10 .

[75]. Reza, K. M., Kurny, A., & Gulshan, F. (2017). Parameters affecting the photocatalytic degradation of dyes using TiO_2: a review. *Applied Water Science*, *7*, 1569-1578 .

[76]. Maki, L. K., Maleki, A., Rezaee, R., Daraei, H., & Yetilmezsoy, K. (2019). LED-activated immobilized Fe-Ce-N tri-doped TiO_2 nanocatalyst on glass bed for photocatalytic degradation organic dye from aqueous solutions. *Environmental Technology & Innovation*, *15*, 100411 .

[77]. Luque-Morales, P. A., Lopez-Peraza, A., Nava-Olivas, O. J., Amaya-Parra, G., Baez-Lopez, Y. A., Orozco-Carmona, V. M., Garrafa-Galvez, H. E., & Chinchillas-Chinchillas, M. d. J. (2021). ZnO semiconductor nanoparticles and their application in photocatalytic degradation of various organic dyes. *Materials*, *14*(24), 7537 .

[78]. Rajkumar, R., Ezhumalai, G., & Gnanadesigan, M. (2021). A green approach for the synthesis of silver nanoparticles by Chlorella vulgaris and its application in photocatalytic dye degradation activity. *Environmental Technology & Innovation*, *21*, 101282 .

[79]. Pachiyappan, J., Gnanansundaram, N., Sivamani, S., Sankari, N. P. B. P., Senthilnathan, N., & Kerga, G. A. (2022). Preparation and characterization of magnesium oxide nanoparticles and its application for photocatalytic removal of rhodamine B and methylene blue dyes. *Journal of Nanomaterials*, *2022* .

[80]. Kumar, R., Barakat, M., Al-Mur, B. A., Alseroury, F. A., & Eniola, J. O. (2020). Photocatalytic degradation of cefoxitin sodium antibiotic using novel BN/$CdAl_2O_4$ composite. *Journal of Cleaner Production*, *246*, 119076 .

[81]. Khezrianjoo, S., Lee, J., Kim, K.-H., & Kumar, V. (2019). Eco-toxicological and kinetic evaluation of TiO_2 and ZnO nanophotocatalysts in degradation of organic dye. *Catalysts*, *9*(10), 871 .

[82]. Mohagheghian, A., Hooshmand Rad, S., Ayagh, K., & Shirzad-Siboni, M. (2022). Photocatalytic Removal of Acid Blue 113 Dye from Aqueous Solutions Using Zinc Oxide-Kaolin Nanocomposite under Visible Light Irradiation. *Journal of Mazandaran University of Medical Sciences*, *32*(209), 146-162.

تصفیه فتوکاتالیستی و مطالعه سینتیک فاضلاب رنگی با نانوذرات اکسید روی سنتز شده

بهنوش خطائی[1*]، فرهاد قادری[2] و فرزاد مساوات[2]

۱- بخش مهندسی عمران، دانشگاه صنعتی اراک، اراک، ایران
۲- بخش مهندسی عمران، دانشگاه صنعتی نوشیروانی بابل، بابل، ایران

ارسال ۲۰۲۴/۰۴/۲۷، پذیرش ۲۰۲۴/۰۶/۲۵

* نویسنده مسئول مکاتبات: b.khataei@arakut.ac.ir

چکیده:

افزایش تعداد کارخانه‌ها، صنعتی شدن زندگی انسان‌ها، و افزایش کاربرد رنگ‌های صنعتی منجر به افزایش تولید فاضلاب رنگی و درنتیجه آلودگی محیط زیست شده‌است. تخلیه فاضلاب حاوی رنگ، که اغلب سرطان‌زاست، تهدید جدی برای موجودات زنده می‌باشد. در این تحقیق، روش فتوکاتالیستی (به عنوان یک روش اکسیداسیون پیشرفته) با کاربرد نانوذرات اکسید روی (ZnO) برای تصفیه فاضلاب رنگی حاوی متیلن بلو مورد بررسی قرار گرفت. این نوع نانوذرات ارزان (بر اساس روش سنتز)، فراوان، به آسانی در دسترس و دارای سمیت کم می‌باشند. بدین منظور، نسبت بهینه استات روی به پلی وینیل پیرولیدون (PVP) برای سنتز نانوذرات ZnO ارزیابی شد. به علاوه، اثرات کاهش و افزایش همزمان پارامترهای مستقل (pH، زمان تابش، غلظت متیلن بلو، نسبت استات روی به PVP) بر راندمان فرایند فتوکاتالیستی و مدل سینتیک بررسی گردید. نتایج نشان داد که بهترین راندمان حذف آلاینده (۹۱/۷ درصد) با کاربرد نسبت استات روی به PVP برابر با ۳۳/۶۷ در مدت تابش ۶۰ دقیقه بدست آمد. بنابراین، نسبت کمتر استات روی به PVP، حذف بیشتر رنگ را نتیجه داده است.

کلمات کلیدی: فتوکاتالیست، فاضلاب رنگی، بهینه سازی، سینتیک، اکسید روی.